Letters

Dynamic recovery of austenite in low carbon steel and its relationship to the precipitation of AlN

Before hot rolling low carbon, aluminium-killed steels, aluminium nitride is in solid solution in austenite. Torsional deformation and deformation by hot rolling induce a quick precipitation of aluminium nitride [1, 2]. At slow torsion rate (i.e. below 3.5 rpm), the curves of deformation-torque, or strain-stress, do not have the typical maximum torque at the strain level corresponding to the start of softening processes leading to steady state in flow stress. This signifies that the softening mechanism is predominantly dynamic recovery [3]. It was assumed that such deformation could enhance the precipitation of AlN from supersaturated austenite, as is the case of higher deformation rates when discontinuous precipitation takes place behind the recrystallization front.

After torsional deformation, the presence of AlN was proved by the Beeghly method of chemical analysis both in samples with altered and non-altered austenite grain size, i.e. in recrystallized and non-recrystallized austenite during one revolution of torsional deformation. Consequently, we wish to ascertain if there was a difference in stress-strain behaviour between the austenite containing AlN precipitates at the start of deformation and austenite without such precipitates and containing Al and N in supersatured solution in order to verify the former observation.

A period of linear strain hardening exists in the stress-strain relationship after the start of torsion. This period is followed by a parabolic relationship showing that the strain hardening increase is diminished by the dynamic recovery involving a reduction of dislocation density by mutual annihilations, as cross-slip and climb [4] enable dislocations to bypass the obstacles created by strain hardening.

Low carbon, aluminium-killed steel with 0.08% C, 0.25% Si, 0.36% Mn, 0.073% Al, 0.0102% N by wt, and low impurity content was chosen for the experimental work. Samples were treated to obtain steel with and without AlN precipitates at the start of torsion. Steel with precipitates was obtained as follows: solution treatment for 1 h at 1300°C, quenching in water and precipitation annealing 2 h at 600°C. This treatment should cause the formation of precipitates with medium size nearly 50 Å [5]. Austenite with Al and N in solid solution was obtained by cooling the samples from the solution to the torsion temperature in the furnace of the torsion device. It has been previously proved [1] that the incubation period for precipitation was long enough for deformation to occur before precipitation began in non-strained steel.

The tests were carried out at 1000 and 1100°C where no significant influence of annealing on quantity and size of AlN precipitates was expected during the tests. Torsion speeds were 0.4, 1.2, and 3.5 rpm, mostly the latter. Higher speeds could not be used as they could not be recorded with enough reliability over the initial phase in the deformation-torque curve.

Results are presented in Figs. 1 and 2. After a certain initial period, a parabolic relationship

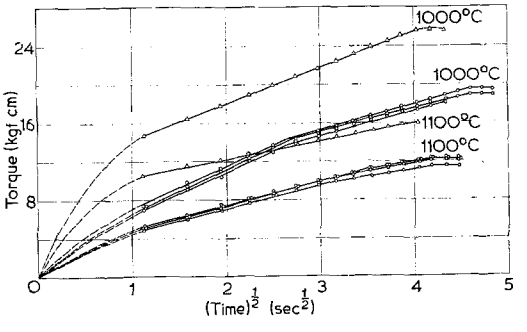

Figure 1 Influence of time (straining at constant rate) on strain hardening (torque). Straining rate = 3.5 rpm. △, austenite containing precipitates; ○, austenite without precipitates.

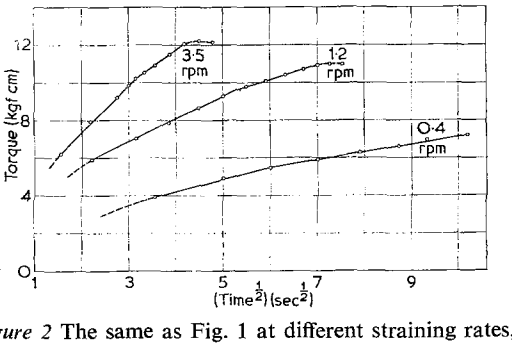

Figure 2 The same as Fig. 1 at different straining rates, temperature = 1100°C.

TABLE I

Strain rate (rpm)	Start of recovery		Change from period A to B	
	Strain	Shear stress (kgf cm^{-2})	Strain	Shear stress (kgf cm^{-2})
0.40	0.30×10^{-2}	69.0	0.91×10^{-2}	97.0
1.2	0.36×10^{-2}	101.0	1.88×10^{-2}	162.0
3.5	0.53×10^{-2}	109.0	2.24×10^{-2}	183.0

is established between the increasing strain, represented as time at constant torsion rate, and the strain hardening in austenite containing precipitates. This dependence shows the effect of the dynamic recovery on strain hardening and is valid until the maximum torque is reached. After this point, steady state is established between the increasing strain and the strain hardening. The relationship is similar in austenite containing aluminium and nitrogen in supersatured solution at the beginning of the torsion, but the parabolic phase shows two different periods, periods A and B, of enhanced recovery which again ends in steady state.

The recovery process is more effective in reducing the strain hardening in period B than in A and is even more effective in the austenite containing AlN precipitates at the start of the deformation. In this case, recovery starts at the highest strain hardening.

It is possible to determine from Fig. 2 the influence of the strain rate on the strain and shear stress [6] where period A of the recovery process changes to B and the recovery process starts. Both values are presented in Table I. Dynamic recovery starts and period A of recovery changes to B at a lower strain hardening when strain rate is also lower. It can be concluded that the dynamic recovery process is influenced by two parameters: the absolute value of strain hardening and the strain rate.

The presence of AlN precipitates simultaneously enhances strain hardening and rate of recovery of the austenite. The first observation could be expected from a general point of view; the second could, at first sight, indicate that the higher recovery rate is related to the higher strain hardening, which could enhance the elimination of dislocation from austenite and provoke earlier attainment of the steady stress-strain state. Using the normal procedure in deformation tests, it is possible to derive from the curves in Fig. 1 the activation energies for the process controlling the recovery of austenite at increasing strain. This process is thermally activated, therefore the difference in kinetics, expressed as the slope of the curves, is connected with the difference in temperature and the activation energy by the Arhenius equation. The derived activation energies are as follows: austenite containing precipitates at the start of deformation: 69.0 kcal mol^{-1}, austenite without precipitates: period A, 68.5 $\pm$ 2 kcal mol^{-1}; period B, 50.0 $\pm$ 1 kcal mol^{-1}.

The difference in the activation energies for recovery between austenite containing precipitates and austenite without precipitates, period A, is not significant. Both values are similar to the activation energy for self diffusion in austenite [7] and show that the recovery is controlled by vacancy motion in austenite. The rate of recovery is, however, higher in austenite containing AlN precipitates at the start of deformation. This suggests that once the recovery has started at a higher strain, the precipitates work as sinks for moving dislocations.

The activation energy is significantly smaller in phase B, suggesting that the recovery process is controlled by a different mechanism which cannot be explained at the present time on the basis of the available data. It is presumed that the start of period B of recovery could be probably related to the start of AlN precipitation and the enhanced recovery resulting from the presence of precipitates in the strained austenite. Precipitation during hot deformation of austenite produces smaller carbonitride precipitates than normal precipitation [8]; a similar effect could be expected for recovery-induced precipitation of AlN. Further experimental work is necessary to clarify this question and find its possible relationship to the recovery process.

Acknowledgement

The author is indebted to the Boris Kidrič Foundation, Ljubljana, Yugoslavia, which supported the investigation.

References

1. F. VODOPIVEC, *Met. Tech.* **1** (1974) 151.
2. *Idem, JISI* **211** (1973) 664.
3. R. A. P. DJAJIC and J. J. JONAS, *ibid* **210** (1972) 256.
4. H. P. STÜWE, *ISI Pub.* **108** (1968) 1.
5. T. GLADMAN, I. D. MCIVOR and F. B. PICKERING, *JISI* **210** (1972) 653.
6. Y. OHTAKAWA, T. NAKAMURA and S. SAKUI, *Trans. ISIJ* **12** (1972) 36.
7. H. J. MCQUEEN, *J. Metals* **20** (1968) 31.
8. A. LE BON, J. ROFES-VERNIS and C. ROSSARD, *Mem. Sci. Rev. Met.* **70** (1973) 577.

Received 16 September
and accepted 2 December 1974

V. VODOPIVEC
Institute of Metallurgy,
Ljubljana, Yugoslavia

The role of twin boundary/grain-boundary intersections on microcracking behaviour of AISI 304 stainless steel deformed in slow tension and creep at 650°C

Studies of intergranular crack formation in metals at elevated temperatures have shown that triple points may provide both preferential sites for the nucleation of cracks and barriers to their propagation [1-5]. Although it has been shown that the growth of cracks originating at grain-boundary triple junctions may be arrested or interrupted at twin boundary/grain-boundary intersections [6, 7] relatively little is known concerning the influence of these intersections on the crack propagation process is austenitic stainless steel.

Recent work has shown evidence for the formation of cracks and cavities along twin boundaries in 304 stainless steel [8]. These results suggest that the twin boundaries may behave in a manner similar to grain boundaries under the proper conditions.

The purpose of this communication is to report quantitative observations concerning the influence of twin boundary/grain-boundary intersections (hereafter referred to as TGI) on the intergranular cracking behaviour in AISI 304 stainless steel deformed in the slow tension and creep rupture modes at a test temperature of 650°C. The experimental test data and the chemical analysis of the alloy are available in [5].

Fig. 1 shows the crack morphology that will be used in this analysis. In addition to those cracks whose lengths, in terms of grain-boundary facets, fall in the interval $l \leqslant 2$ and are not terminated at TGI [5], a non-negligible number of triple-point cracks were also observed to terminate at TGI (See Fig. 1c and e). Cracks not associated with triple junctions but associated with TGI's were also observed. These cracks are shown in Fig. 1i to k. Secondary cracks [9] are defined as those which are not associated with triple points (Fig. 1g to k). The cracks in both these groups were, therefore, evaluated in a manner similar to that used for the triple-point cracks previously discussed [10]. Relatively few cracks with lengths $l > 2$ were observed to terminate at TGI [10].

The distribution of triple-point cracks terminated at TGI's, as well as secondary cracks associated with TGI's, is plotted in Fig. 2 as a function of deformation rate. It is apparent that both the intergranular cracks related to TGI's and the secondary cracks increase with decreasing deformation rate (i.e. decreasing stress levels). This observation is consistent with the overall intergranular crack results for these specimens where triple junctions are involved [5] and suggests a correlation with the tendency for strain associated with grain-boundary sliding.

There is a strong indication that the propagation of triple-point cracks may be interrupted at TGI's. This is mainly based on the observation that there are non-negligible number of triple-point cracks which occupy sites between triple points and TGI (as shown in Figs. 1c and e, and 2). Although it is difficult to visualize the actual cracking process, it can be safely assumed that the intergranular cracks have a greater tendency to nucleate at or near the triple point and then proceed toward the TGI and the next triple point. This circumstance may be explained by the fact that the surface energy [11] and stress concentration due to the applied stress at triple junctions are higher than those at TGI's. The majority of cracks observed are triple-point cracks which again supports this idea. Fig. 3a shows the angular incidence with respect to the applied stress of triple-joint cracks which are filled between the triple junction and TGI (Fig. 1c). Cracks with a length of less than one boundary facet are plotted in Fig. 1c. The